JACS
JOURNAL OF THE AMERICAN CHEMICAL SOCIETY
Article
Cite This: J. Am. Chem. Soc. 2019, 141, 17189−17197
pubs.acs.org/JACS

# Nicking-Assisted Reactant Recycle To Implement Entropy-Driven DNA Circuit

Cheng Zhang,[*,†,‡] Zhiyu Wang,[§,◆] Yan Liu,[∥,⊥,◆] Jing Yang,[#,◆] Xinxin Zhang,[#] Yifan Li,[#] Linqiang Pan,[§] Yonggang Ke,[*,▽,○] and Hao Yan[*,∥,⊥]

[†]School of Electronics Engineering and Computer Science, Peking University, Beijing 100871, China
[‡]College of Medical Technology, Peking University Health Science Center, Beijing 100871, China
[§]Huazhong University of Science and Technology, Wuhan 430074, Hubei China
[∥]Center for Molecular Design and Biomimetics, The Biodesign Institute, and [⊥]School of Molecular Sciences, Arizona State University, Tempe, Arizona 85287, United States
[#]School of Control and Computer Engineering, North China Electric Power University, Beijing 102206, China
[▽]Wallace H. Coulter Department of Biomedical Engineering, Georgia Institute of Technology and Emory University, Emory University School of Medicine, Atlanta, Georgia 30322, United States
[○]Department of Chemistry, Emory University, Atlanta, Georgia 30322, United States

Supporting Information

**ABSTRACT:** Synthetic catalytic DNA circuits are important signal amplification tools for molecular programming due to their robust and modular properties. In catalytic circuits, the reactant recycling operation is essential to facilitate continuous processes. Therefore, it is desirable to develop new methods for the recycling of reactants and to improve the recyclability in entropy-driven DNA circuit reactions. Here, we describe the implementation of a nicking-assisted recycling strategy for reactants in entropy-driven DNA circuits, in which duplex DNA waste products are able to revert into active components that could participate in the next reaction cycle. Both a single-layered circuit and multiple two-layered circuits of different designs were constructed and analyzed. During the reaction, the single-layered catalytic circuit can consume excess fuel DNA strands without depleting the gate components. The recycling of the two-layered circuits occurs during the fuel DNA digestion but not during the release of the downstream trigger. This strategy provides a simple yet versatile method for creating more efficient entropy-driven DNA circuits for molecular programming and synthetic biology.

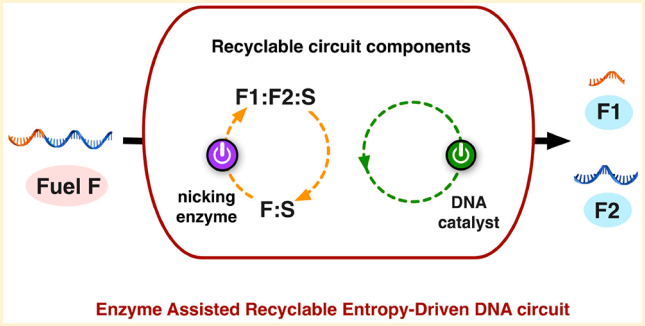


## INTRODUCTION

Molecular interactions based on Watson−Crick nucleic acid base pairing have allowed scientists to design various self-assembly systems, including complicated nanostructures,[1−3] nanomechanical devices,[4−6] and signaling circuits.[7−12] In particular, DNA circuits play a critical role in signal amplification and information regulation in engineered biomolecular systems. Recently, substantial efforts have been taken to design more advanced and complex synthetic circuit systems for the construction of increasingly reliable, efficient, and intricate molecular signal pathways.[7−13] In natural DNA networks, the programmable DNA circuits are usually regulated by both proteins and nucleic acids.[14−16] Accordingly, the synthetic DNA circuits have been used to transmit complex information via two main catalysis mechanisms: enzyme-dependent DNA cascades[17−25] and entropy-driven DNA catalytic reactions.[26−32]

In particular, entropy-driven circuits are attractive due to their catalytic ability, signal amplification, and programmable networks. After the seminal work by Zhang et al.,[30] entropy-driven DNA circuits have been widely used for molecule detection,[33,34] logic operations,[35−37] nanostructure formation,[38,39] and molecular engineering.[4,40] However, in the canonical entropy-driven circuit, the gate components become waste after being used only once, which limits the efficiency of the signal-generating catalytic reaction. Therefore, it is desirable to develop simple recycling methods to implement catalytic DNA circuits without depleting the gate component.

There have been efforts to create DNA circuits that can recycle gate components.[41−43] In these systems, the renewable circuits were created by additional DNA strand displacement reactions, through which the gate components could revert to

Received: July 15, 2019
Published: September 20, 2019






DOI: 10.1021/jacs.9b07521
J. Am. Chem. Soc. 2019, 141, 17189−17197

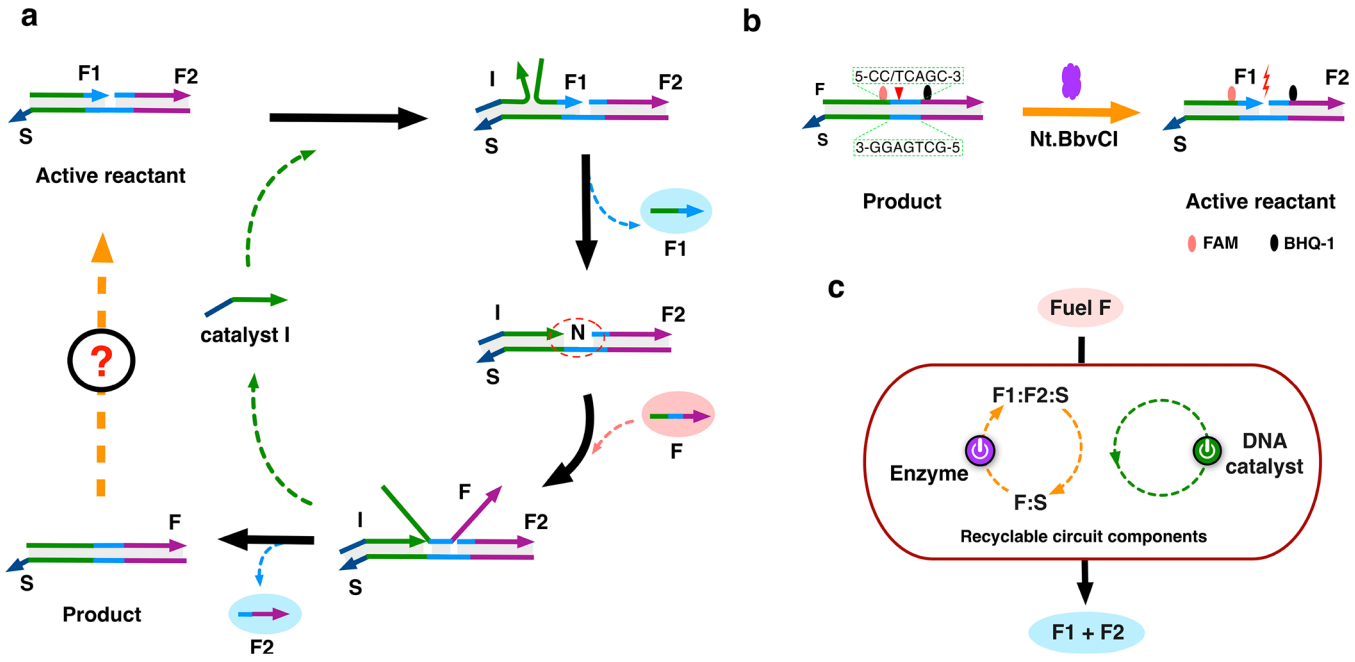


**Figure 1.** Nicking-assisted recyclable entropy-driven DNA circuit designs. (a) A schematic of the C1 DNA circuit. The question mark indicates the desired step by which to make the circuit recyclable. (b) The enzymatic nicking digestion reverts the gate product F:S to an active reactant F1:F2:S. (c) A simplified schematic diagram of the C1 circuit.

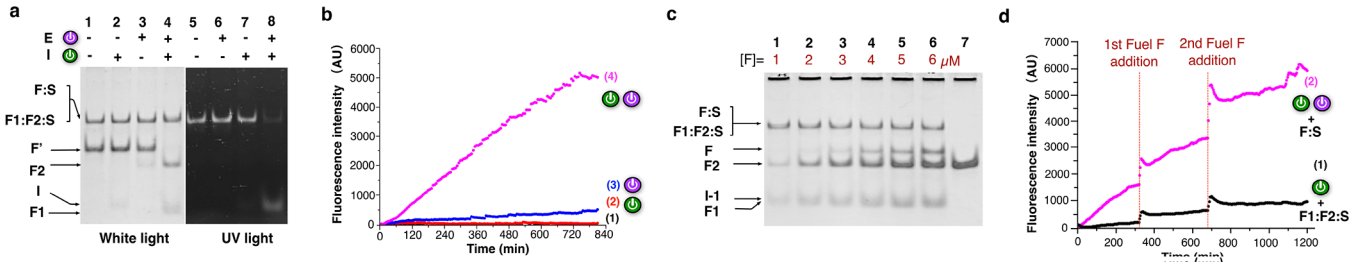


**Figure 2.** Analysis of the C1 circuit. (a) PAGE gel results of the C1 circuit operations (12% gel): lane 1, no catalyst; lane 2, I; lane 3, E; lane 4, I + E. Gel results from lanes 1−4 were detected with Stains-All under room light, while the results from lanes 5−8 were detected under UV light without staining. (b) The analysis of the C1 circuit via a fluorescence assay: trace 1, no catalyst; trace 2, I; trace 3, E; trace 4, I + E. The detection time interval was 6 min. (c) The PAGE gel results from experiments completed by increasing the concentrations of the fuel F ([F:S] = 0.8 $\mu$M). (d) The control experiment with sequential additions of the F fuel: trace 1, F1:F2:S + I reactants; trace 2, F:S + I + E reactants.

their original state. However, additional DNA reactants inevitably increase the complexity of these modified DNA circuits. Recently, enzyme-mediated reactions (e.g., RNAP/RNase,[44] PEN DNA toolbox,[13,25,45] and nicking enzymes[46,47]) proved to be effective methods to achieve the reactant recycling DNA/RNA circuits. These advancements suggest that new entropy-driven DNA circuits with improved recyclability may be developed by the incorporation of enzymatic reactions.

In this study, we introduced a nicking-assisted reactant recycling strategy (NARR) to create an entropy-driven DNA circuit. The duplex gate components (generated from the last circuit reaction) can revert back to their original active state with the aid of a nicking enzyme digestion. The newly nicked gate component can then participate in the next circuit reaction. The experimental results demonstrate that the single-layered catalytic circuit can be used to consume the excess fuel DNA strand without depleting the gate component. In addition, the recycling of the two-layered circuits occurs during the fuel DNA digestion process but not during the release of the downstream trigger and signal.

## RESULTS AND DISCUSSION

**Design of Nicking-Assisted Strategy To Implement Entropy-Driven C1 Circuit.** The design details of a canonical entropy-driven DNA circuit are displayed in Figure 1a. In the reaction, the DNA initiator strand I first triggers a strand displacement to replace the F1 strand with an active F1:F2:S DNA gate complex. Accordingly, an I:F2:S metastable structure, containing an exposed 4 nt single-stranded domain, is generated and contains an N in the middle of the duplex complex. This metastable structure allows for one full-length F fuel strand to simultaneously displace both of the I and F2 strands, thus leading to the recycling of the DNA catalyst I and the generation of an F:S product. The F:S product will accumulate over time. The circuit reaction will stop when any one of the two reactants, the F fuel or the F1:F2:S gate, is completely consumed (whichever comes first). However, a high recyclability reaction rate can be achieved if an approach to revert the F:S gate product into the active F1:F2:S reactant exists (the question mark in Figure 1a). The recycling will stop once the F fuel is used up (after all of the F fuel is converted into F1 and F2).



DOI: 10.1021/jacs.9b07521
J. Am. Chem. Soc. 2019, 141, 17189−17197

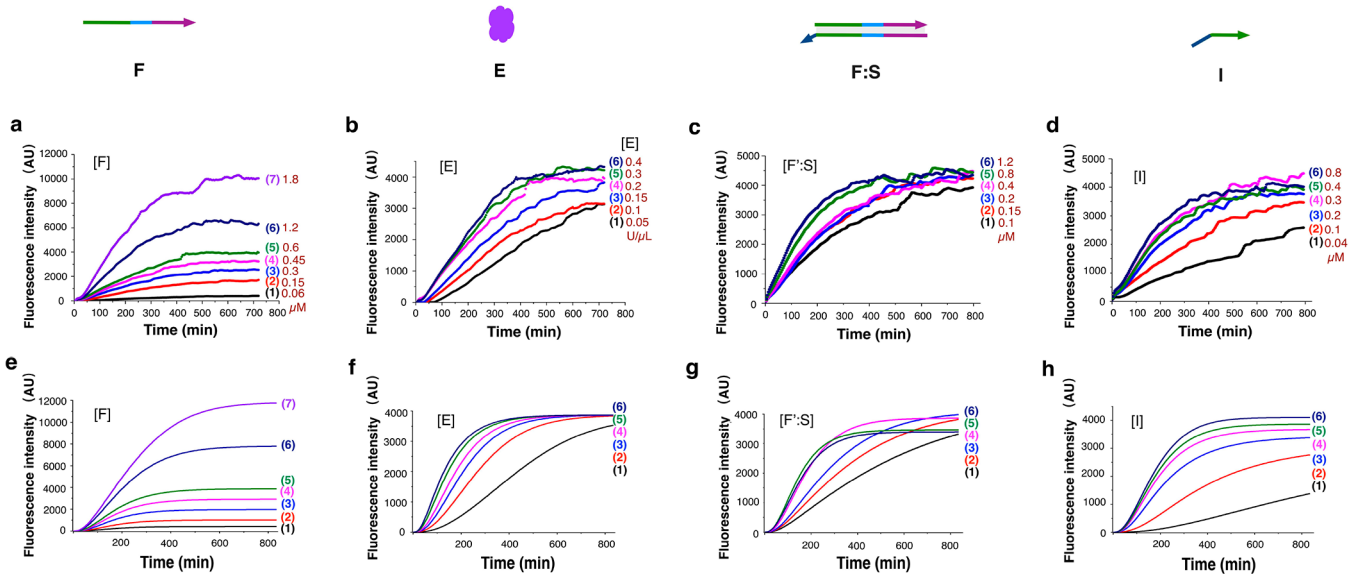


**Figure 3.** Analysis of the reactants' catalytic functions in the C1 circuit. (a–d) Fluorescence results of the fluorescence assay experiments with varying concentrations of the F fuel strand, E enzyme, F:S reactant, and catalyst I, respectively, while the concentrations of the other components were kept constant. For panels b–d, the concentrations of F used were 0.6 $\mu$M. The detection time interval was 4 min. Experimental details can be found in section S12 of the Supporting Information. (e–h) Simulation results.

With the NARR strategy, a site-specific single-stranded nicking digestion was utilized to repeatedly create the reactant necessary for the recycling process (Figure 1b). A specific 7 bp nicking site was added to the middle of the F:S product. After the nicking process was completed, by using the Nt.BbvcI (E) enzyme, a newly formed F1:F2:S nicked complex was created that could then be used in the next reaction cycle. Thus, during the reaction, the circuit consumes the excess F fuel strands without depleting the gate component. The enzyme-assisted entropy-driven C1 circuit is summarized in Figure 1c, where the inputs and outputs of the reaction is the DNA F fuel and the F1 and F2 DNA products, respectively.

**Analysis and Regulation of the C1 Circuit.** The C1 circuit reaction (Figure 1c) was first confirmed with a native PAGE gel electrophoresis (Figure 2a). The reactions during the gel assay included an excessive amount of the F fuel strand and a limited amount of the F:S complex. The recyclability of the C1 circuit could be determined on the basis of the complete consumption of the F fuel strand. Lane 1 lacked both catalysts. Also, no consumption of the F fuel strand was observed in lane 1, indicating that the reaction did not occur. When either I or E was present, a strong band for the F fuel strand (in lane 2 or 3, respectively) was observed. These bands indicated that the recycling circuit was not activated. However, when both I and E were introduced simultaneously, the F fuel strand band completely disappeared. Accordingly, the F1 and F2 products appeared (lane 4), demonstrating that the circuit reaction had occurred. To better verify the reaction, an F:S labeled fluorescence-dye and an unlabeled F′ fuel strand was used in lanes 5–8. As expected, when both I and E were present (lane 8), the fluorescent gel bands arising from the initial F:S reactant disappeared, while the fluorescent gel band arising from the F1 product appeared, thus proving that the recycling reaction occurred. The operation of the C1 circuit was also monitored by its fluorescence intensity with a time-course study (Figure 2b). The F fuel strand was labeled with a fluorophore (FAM) and a quencher (BHQ-1) on either side of the nicking site, each separated by a 13 nt (~4.5 nm) distance. An increase in the fluorescence intensity was expected to occur if the fluorophore and the quencher were separated from each other. In Figure 2b, a significant increase in the fluorescence was observed following the addition of the I and E catalysts (trace 4). However, no significant increase in the fluorescence was observed when introducing none or either of the catalysts alone (from traces 1–3).

To further analyze the recyclability of the cycling NARR circuit reactions, a series of control experiments were conducted. First, native PAGE gel experiments were performed by varying the concentrations of the F fuel strand, E enzyme, initial gate component (F:S), and the catalyst I, respectively. As shown in Figure 2c, when there was an increase in the concentration of the F fuel strand from 1 to 6 $\mu$M, with a constant [F:S] = 0.8 $\mu$M, the overall production of F1 and F2 increased accordingly. The results confirmed that a small amount of the F:S gate could instigate the consumption of a large amount of the excess F fuel. Meanwhile, we also tested how the outcome of the reaction changed with increasing concentrations of the E enzyme, the initial reactant (F:S), and the DNA catalyst I, respectively [Figure S3b–d, Supporting Information (SI)]. Here, the recyclable property of the F:S gate reactant could be determined by measuring the turnover number, which is defined as the number of fuel strands consumed per F:S. For example, in lane 4 of Figure S3c (SI), 2.5 pmol of the F:S reactant could instigate the consumption of 28.25 pmol of the F fuel strand. In this case, the turnover number was 11.3 (determined with ImageJ), indicating a strong catalytic capability. More calculations of the turnover numbers can be found in section S3.2 of the Supporting Information. We also observed a stepwise jump of the fluorescence signal when additional aliquots of the F fuel were introduced to the reaction (Figure 2d). The quick consumption of the newly added F fuel further confirmed the recyclability of the circuit reaction.

As reported in a previous study, when reducing the concentrations of a recyclable DNA reactant that acts as a catalyst within a reasonable range, only the reaction rate is


DOI: 10.1021/jacs.9b07521
J. Am. Chem. Soc. 2019, 141, 17189–17197

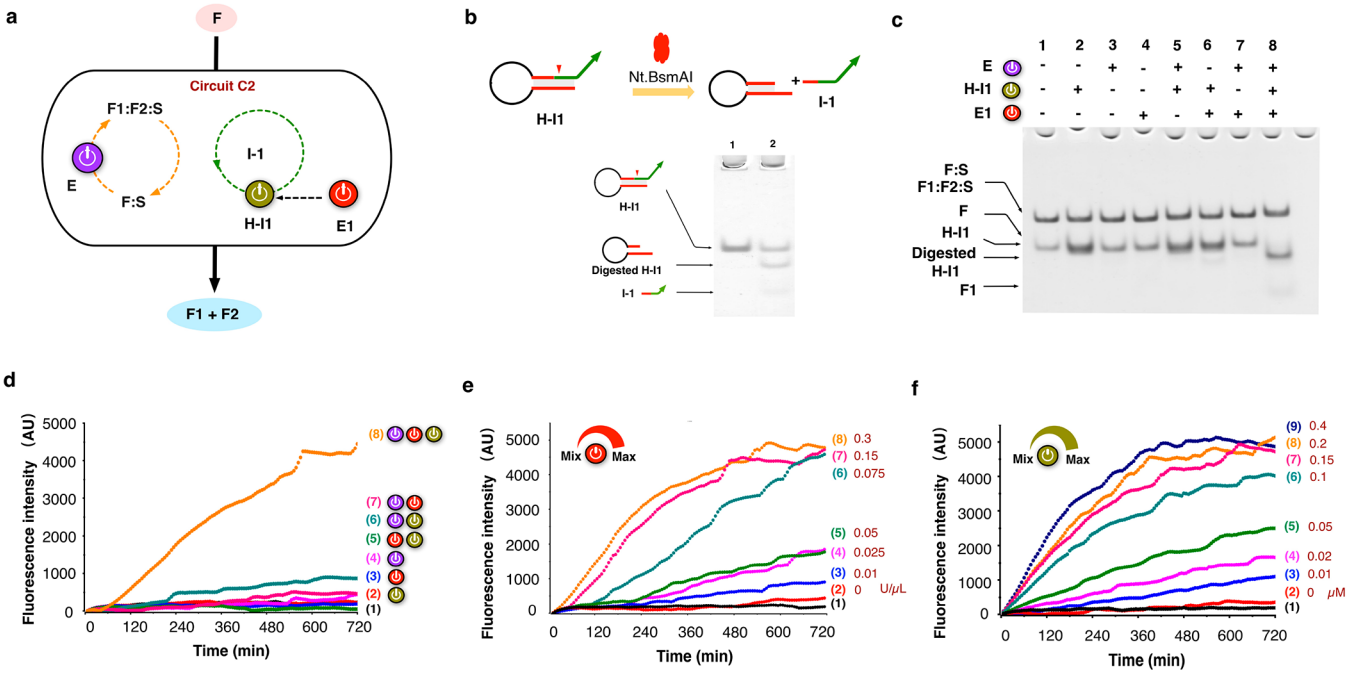


**Figure 4.** C2 circuit with a catalyst protection and release strategy, using a hairpin H-I1 structure to hide the I-1 catalyst and a second nicking enzyme, E1, for its release. (a) The simplified schematics of the C2 circuit. (b) The design and gel results of the catalyst release. (c) PAGE results of the operation of the C2 circuit. The gel was stained with Stains-All. (d) Fluorescence assay of the operation of the C2 circuit. Fluorescent assays determining the regulating functions of the E1 (e) and the H-I1 hairpin (f) by varying the concentrations of the E1 or H-I1, respectively. The detection time interval was 6 min. The experimental details can be found in sections S5 and S12 of the Supporting Information .

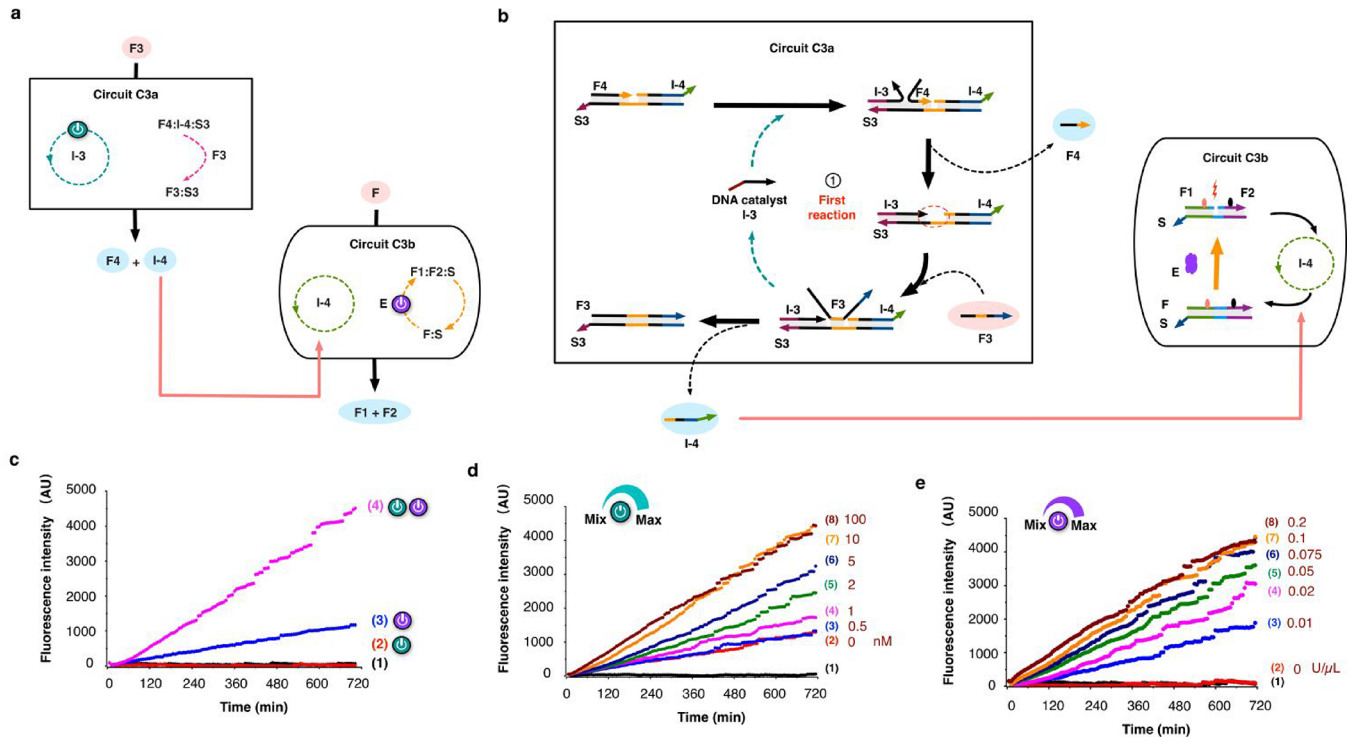


**Figure 5.** A two-level cascading C3 circuit. The simplified schematics (a) and detailed reaction of the C3 circuit (b). (c) The analysis of the C3 circuit using a fluorescent assay: trace 1, no catalyst; trace 2, I-3; trace 3, E; trace 4, I-3 + E. Fluorescence results of the reactions with varying concentrations of the I-3 DNA catalyst (d) and the E enzyme (e). The detection time interval was 6 min. More information can be found in sections S6 and S12 of the Supporting Information.

decreased, but not the final equilibrium state.[28] To analyze the catalytic abilities of the circuit reactants, each reactant was studied individually by gradually reducing its concentration and monitoring its fluorescence output (Figure 3). When the concentration of the consumable F fuel strand was reduced, the final fluorescence intensities decreased accordingly (Figure



DOI: 10.1021/jacs.9b07521
J. Am. Chem. Soc. 2019, 141, 17189−17197

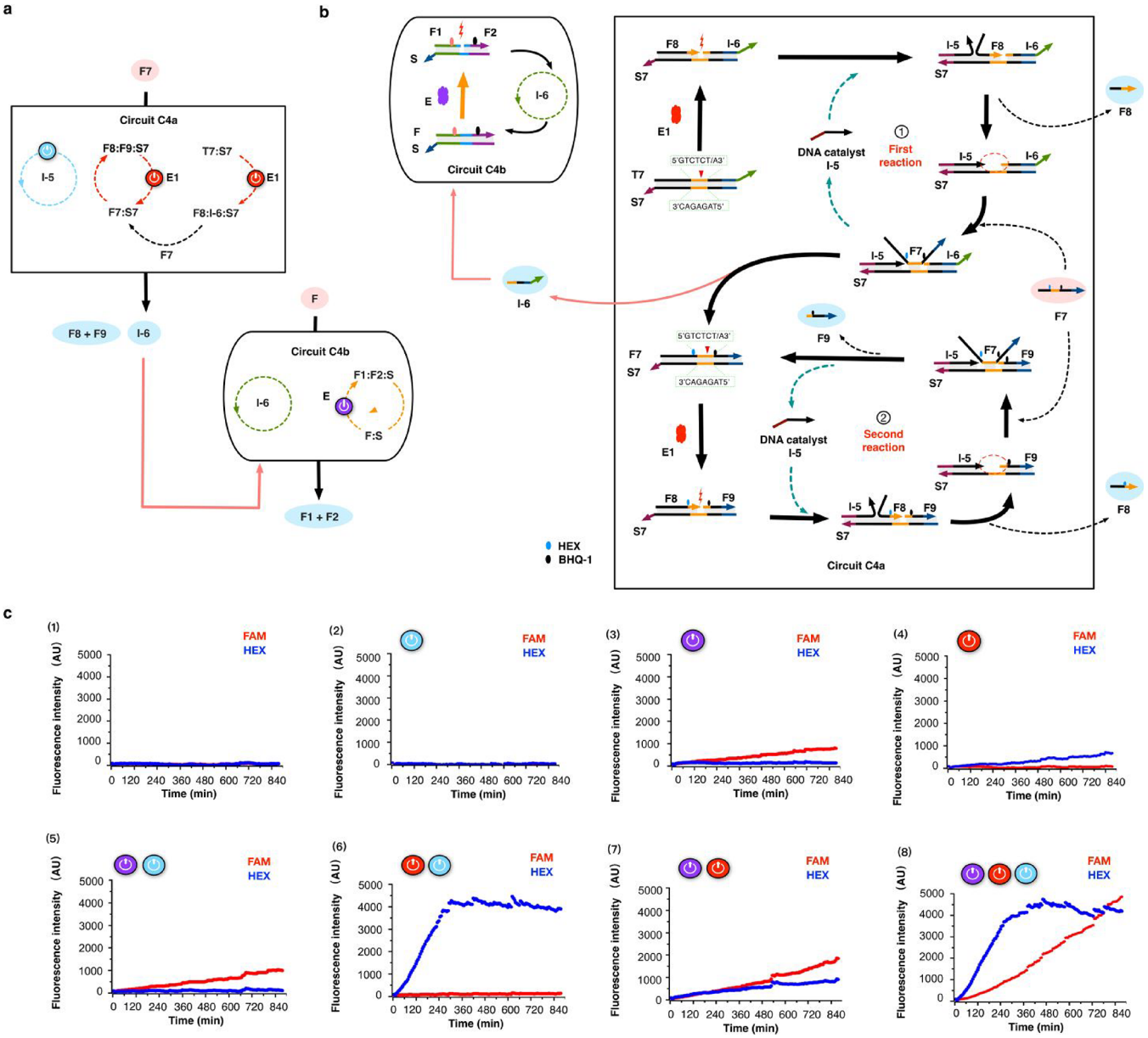


**Figure 6.** Hierarchical cascading C4 circuit. (a) The schematics of the C4 circuit. (b) The detailed reaction of the C4a subcircuit. (c) Fluorescence results depicting the different trigger modes: (1) no catalyst, (2) I-5, (3) E, (4) E1, (5) E + I-5, (6) E1 + I-5, (7) E + E1, and (8) E + E1 + I-5. More information can be found in sections S7 and S12 of the Supporting Information.

3a). However, for the recyclable reactants (the E enzyme, initial gate component F:S, or catalyst I), the final fluorescence intensities did not significantly change in correspondence with the variation in the concentrations of the reactant (Figure 3b–d). The catalytic abilities were analyzed in detail by comparing the F (nonrecyclable) reactants and the F:S (recyclable) reactants. When the concentration of the nonrecyclable F fuel was reduced 10-fold, from 0.6 to 0.06 $\mu$M (Figure 3a), the final fluorescence intensity decreased about 10-fold as well. In contrast, as the concentration of the recyclable gate component F:S was reduced 12-fold from 1.2 to 0.1 $\mu$M (Figure 3c), no significant change in the final fluorescence intensity was observed. The strong catalytic ability of the recyclable F:S is reflected by this result. In addition, simulation results were consistent with the experimental results (Figure 3e–h). More details can be found in section S4 of the Supporting Information.

**A C2 Circuit with a Catalyst Release Strategy.** A C2 circuit was designed by using two enzyme regulators: E (Nt.BbvCI) and E1 (Nt.BmsAI) (Figure 4a). Here, a catalyst protection and release strategy was employed to control the activity of the I-1 DNA catalyst. Specifically, the I-1 DNA catalyst initially hides in the structure of the H-I1 DNA hairpin and it can be released as an active catalyst after the E1 enzyme digestion (Figure 4b). Clearly, the two enzymes play different roles in the C2 circuit, where E catalyzes the recycling of the reactant and E1 controls the activity of the I-1 DNA catalyst.

The reactions were first analyzed with a native PAGE (Figure 4c). In the absence of any one of the three inputs, the reaction will not proceed and the F fuel strand will not be consumed (lanes 1–7). Only when all three inputs were present simultaneously was the reaction activated. In this case, the complete consumption of the F fuel strand and the H-I1 hairpin occurred (lane 8). A fluorescence assay was also used



DOI: 10.1021/jacs.9b07521
J. Am. Chem. Soc. 2019, 141, 17189–17197

to analyze the C2 circuit (Figure 4d). Similarly, when all three inputs were present, a significant increase in the fluorescence signal was obtained (trace 8). Notably, some leakages were observed when the E enzyme was introduced into the reaction (e.g., trace 6, triggered by the E enzyme and the H-I1 hairpin). The leakages may be attributed to the insufficient protection of the hidden I-1 DNA catalyst in the hairpin, which could result in the activation of a nicked F1:F2:S. A nicked F1:F2:S is a product that occurs in the presence of the E enzyme. Although the leakage occurred in the enzyme-assisted circuit reactions, the leakage could potentially be reduced by using some of the more recently developed strategies, such as shadow cancellation,[48] localization,[49] or toehold clamps.[50] Finally, the regulating effects of the E1 enzymes and the H-I1 hairpin on the circuit reaction were also analyzed with the use of fluorescence assays (Figure 4e,f).

**A Two-Layered C3 Cascading Circuit.** To achieve cascading control over the nicking-assisted circuit operations, a two-layered C3 circuit was developed. This circuit was also controllable via two catalysts: an I-3 DNA catalyst and an E enzyme (Nt.BbvCI) (Figure 5a). The C3 circuit was composed of two individual subcircuits: an upstream C3a subcircuit and a downstream C3b subcircuit. These circuits served as the initiating and the reporting modules, respectively (Figure 5a). Here, the upstream C3a subcircuit was designed as a canonical entropy-driven circuit to function without enzymatic assistance. However, the downstream C3b subcircuit was a catalytic circuit that functions with the assistance of an E enzyme. The I-3 DNA catalysts were designed as inputs that could activate the C3a subcircuit. The I-4 DNA catalyst, that targets the downstream C3b subcircuit, was protected inside the initial F4:I-4:S3 complex, to avoid directly triggering the downstream C3b subcircuit (Figure 5b). (Note: the F3 fuel contains an incomplete I-4 sequence and is thus unable to trigger the downstream C3b subcircuit.)

In the upstream C3a subcircuit (reaction ①, Figure 5b), the I-3 catalyst may cause the preprotected I-4 catalyst to be released. The release of the I-4 catalyst would then trigger the downstream C3b subcircuit, which would result in the generation of a F3:S3 product that is created from the consumption of the F3 fuel. Here, the recycling of the gate reactant does not occur in the upstream C3a subcircuit due to the depletion of the initial F4:I-4:S3 gate. Hence, to avoid directly triggering the downstream C3b subcircuit, the F3 must not contain the I-4 catalyst in its tail domain (colored green in Figure 5b). As a result, the original F4:I-4:S3 gate cannot be recovered by nicking the F3:F3 product with a nicking enzyme. The released I-4 catalyst plays a dual role as both a catalyst in the C3b subcircuit and a cascading messenger to connect the two subcircuits. During the cascading circuit reaction, both the F and F3 fuel strands were consumed. The nicking-assisted reactant recycling process was only performed in the downstream C3b subcircuit, whereas both the E enzyme and the released I-4 catalyst served as regulators to control the C3b subcircuits (Figure 5a,b).

In the fluorescence assay, only when both catalysts, E and I-3, were introduced was a significant fluorescent increase observed (Figure 5c, trace 4). However, in the absence of any one of the regulators, no significant increase in the fluorescence intensity was observed. Nevertheless, a signal leakage was observed when only the E enzyme was introduced (trace 3). This signal leakage may be attributed to the zero-toehold leak reaction that occurs in the circuit.[30] Once a small amount of I-4 leaks, it will trigger a larger output, resulting in significantly greater fluorescence leakages. Finally, experiments of varying concentrations of I-3 and E were also conducted to confirm their roles in regulating the cascading C3 circuit (Figure 5d,e).

**Hierarchical Control of a Two-Layered C4 Circuit.** A two-layered hierarchical C4 circuit was also constructed and controlled by three regulators: two nicking enzymes, E (Nt.BbvCI) and E1 (Nt.BsmAI), and an I-5 DNA catalyst (Figure 6a). The C4 circuit possessed two subcircuits: an upstream C4a subcircuit and a downstream C4b subcircuit, with two reporters that had been labeled with the HEX (fuel DNA F7) and FAM (fuel DNA F) fluorophores, respectively (Figure 6b). Here, both of the C4a and C4b subcircuits were designed as enzyme-regulators, and E1 and E nicking enzymes were used, respectively. Meanwhile, an I-5 DNA catalyst was an input that was used to initiate the C4a subcircuit, while a I-6 DNA catalyst was used to target the downstream C4b subcircuit. However, I-6 catalyst was preprotected in a T7:S7 gate complex, to avoid directly triggering the downstream C4b subcircuit. (Note: the F7 fuel contains an incomplete I-6 sequence and, thus, cannot trigger the downstream C4b subcircuit).

In the upstream C4a subcircuit, reaction ① is first activated by the E1 enzyme digestion to produce an active F8:I-6:S7 product (Figure 6b). Subsequently, with the help of the I-5 catalyst, the entropy-driven reaction was accomplished by consuming the F7 fuel to release the I-6 catalyst and produce the S7:F7 product. The I-6 catalyst could then serve as a connector to trigger the downstream C4b subcircuit, which is similar to the C1 circuit. Meanwhile, the newly generated F7:S7 could serve as a gate reactant to initiate the recyclable circuit reaction ②, where the F7 fuel (modified with HEX/BHQ1) could be continuously consumed to amplify the HEX fluorescence signal of the upstream C4a subcircuit. During the two-layered C4 circuit reaction, both the F and F7 fuel strands were consumed. Due to the hierarchical control arising from the E and E1 enzymes, the two-level circuit reaction could be selectively regulated to give fluorescence signals in the FAM or HEX channels.

Notably, the upstream C4a subcircuit has two functions: (1) releasing the downstream I-6 catalyst in reaction ① and (2) amplifying the fluorescence signal by continuously digesting the F7 fuel in reaction ②. Here, the enzyme-assisted recyclability of the C4a subcircuit was performed only during the fuel DNA digestion process but not during the release of the downstream trigger signal.

In the fluorescence assay, when any one or two of the enzyme regulators were used, no significant increase in the downstream FAM fluorophore signal was observed (in Figure 6c, panels 2−7). However, when all three regulators were present at the same time, a significant increase in the fluorescence of the FAM and HEX fluorophores was obtained (panel 8). Interestingly, when only the E1 and I-5 catalysts were present, a significant increase in the HEX fluorophore signal was obtained, while no FAM fluorophore signal was observed (panel 6). An explanation for this is that the absence of the E enzyme only hindered the downstream C4b subcircuit. However, the upstream C4a subcircuit could still be activated by the E1 catalyst and result in an increase in the HEX fluorophore signal. Such a selective fluorescent signal increase confirms that a hierarchical regulation of the C4 circuit does indeed occur. Moreover, the differences in the kinetic reaction rates can be observed by comparing the HEX


DOI: 10.1021/jacs.9b07521
J. Am. Chem. Soc. 2019, 141, 17189−17197

and the FAM signals in panel 8. Clearly, the HEX signal representing the upstream C4a subcircuit had a faster reaction rate than that of the FAM signal representing the downstream C4b subcircuit. This result is consistent with the hierarchical cascading circuit design. More data about the C4 circuit can be found in Figures S10–S12 of the Supporting Information.

In addition, C5 and C6 are some alternative catalytic circuits that were created on the basis of the NARR strategy. These circuits were constructed to further test the scalability and diversity of the enzyme-assisted entropy-driven circuit reactions (see sections S8 and S10, SI). To further explore the nicking-assisted strategy, we also designed a cascading C7 circuit that was controlled by up to four inputs: three enzymes, E (Nt.BbvCI), E1 (Nt.BsmAI), and E2 (Nb.BtsI), and an H-I3 hairpin DNA (Figure S20, SI). It was found that significant increases in the fluorescence took place only when all four regulators were present simultaneously (Figure S22, SI).

## CONCLUSIONS

Our study provides a nicking-assisted reactant recycling method that can be used to create an entropy-driven DNA circuit. The experimental results verified that enzyme-assisted recyclability in single-layered circuits could be achieved, whereby a gate DNA product could be reverted into its original active state and repeatedly participate in a chemical reaction. In addition, the two-layered DNA circuits were also established with hierarchical and multiplex rules. It was demonstrated that the NARR strategy improved the recyclability of the entropy-driven DNA circuit.

In the canonical entropy-driven DNA circuit, a "single-use" gate architecture caused an irreversible depletion of the gate component, thus limiting the cycling of a reaction. Multiple strategies have been developed to achieve gate architecture recycling, such as renewable circuits and time-responsive circuits.[41−43] Renewable circuits have the ability to revert to their original gate states,[43] and the time-responsive circuits can dynamically change their outputs when the inputs change.[42] Here in this study, the recyclable single-layered circuit adopts the renewable strategy, assisted not only by the entropy-driven strand displacement reaction but also by a nicking enzyme. Different from the multicycle time-responsive circuits, the enzyme-assisted circuit reported here cannot dynamically produce output signals in response to changing inputs.

In the catalytic circuits, it should be noted that the recyclability is different in the single- and two-layered DNA circuits. Specifically, in the two-layered C4 circuit, the recyclability is performed only during the digestion of the fuel DNA but not during the downstream trigger signal release. However, in the single-layered C1 circuit, the gate product can be repeatedly reverted into an active reactant without depleting the gate component. Although the gate recycling is limited in the two-layered C4a circuit, the enzyme-assisted strategy is still useful for performing various functions. For example, the use of different enzymes provides us with the ability to hierarchically control the subcircuits. Meanwhile, the enzyme-assisted strategy allows for a continuous digestion of the fuel in order to amplify the fluorescence signal, thus enabling us to independently monitor the operation of the individual subcircuits in real time. Furthermore, this strategy also creates a new method for achieving a multiplex input rule (e.g., DNA or enzyme or both) for catalytic DNA networks. In the future, the high reactant recyclability in the two-layered circuit may be further enhanced by taking advantage of unique chemical modifications or a new DNA catalyst protect/release strategy.

The developed NARR strategy can potentially be used in biosensing, molecular signaling, nanorobotics, and disease diagnostics. We believe the strategy will become more widely applied in DNA nanotechnology and DNA computing due to its ability to imbue DNA circuits with more controllability and complexity.

## ASSOCIATED CONTENT

### Supporting Information

The Supporting Information is available free of charge on the ACS Publications website at DOI: 10.1021/jacs.9b07521.

Details of reaction schematics and the reaction kinetic simulations, calculation of turnover number, design considerations, additional experimental data, and experimental methods and materials (PDF)

## AUTHOR INFORMATION


### Corresponding Authors

*zhangcheng369@pku.edu.cn
*yonggang.ke@emory.edu
*hao.yan@asu.edu

### ORCID

Cheng Zhang: 0000-0002-1131-6516
Zhiyu Wang: 0000-0002-8356-9555
Yan Liu: 0000-0003-0906-2606
Yonggang Ke: 0000-0003-1673-2153
Hao Yan: 0000-0001-7397-9852

### Author Contributions

◆Z.W., Y.L., and J.Y. contributed equally to this work.


### Notes

The authors declare no competing financial interest.

## ACKNOWLEDGMENTS

We thank Kristen Lee and Dr. Victor Pan for the careful review of the manuscript. This work was supported by the National Key R&D Program of China (2017YFE0130600, 2016YFA0501603, and 2017YFE0103900), the National Natural Science Foundation of China (61872002, 61320106005, and 61772214), the Joint Fund of the Equipment Pre Research Ministry of Education (6141A02033607, 6141A02033608), Beijing Natural Science Foundation (4182027) and Beijing Municipal Key R&D Project No. Z151100003915081, and grants from the US National Science Foundation to H.Y and Y.L.

## REFERENCES


(1) Han, D.; Pal, S.; Nangreave, J.; Deng, Z.; Liu, Y.; Yan, H. DNA origami with complex curvatures in three-dimensional space. *Science* **2011**, *332*, 342−346.

(2) Ke, Y.; Lindsay, S.; Chang, Y.; Liu, Y.; Yan, H. Self-assembled water-soluble nucleic acid probe tiles for label-free RNA hybridization assays. *Science* **2008**, *319*, 180−183.

(3) Chidchob, P.; Edwardson, T. G. W.; Serpell, C. J.; Sleiman, H. F. Synergy of two assembly languages in DNA nanostructures: self-assembly of sequence-defined polymers on DNA cages. *J. Am. Chem. Soc.* **2016**, *138*, 4416−4425.

(4) Wickham, S. F. J.; Bath, J.; Katsuda, Y.; Endo, M.; Hidaka, K.; Sugiyama, H.; Turberfield, A. J. A DNA-based molecular motor that can navigate a network of tracks. *Nat. Nanotechnol.* **2012**, *7*, 169−173.




DOI: 10.1021/jacs.9b07521
J. Am. Chem. Soc. 2019, 141, 17189−17197

(5) Kopperger, E.; Pirzer, T.; Simmel, F. C. Diffusive transport of molecular cargo tethered to a DNA origami platform. *Nano Lett.* **2015**, *15*, 2693−2699.
(6) Omabegho, T.; Sha, R. J.; Seeman, N. C. A Bipedal DNA Brownian Motor with Coordinated Legs. *Science* **2009**, *324*, 67−71.
(7) Cherry, K. M.; Qian, L. Scaling up molecular pattern recognition with DNA-based winner-take-all neural networks. *Nature* **2018**, *559*, 370−376.
(8) Zhang, D. Y.; Seelig, G. Dynamic DNA Nanotechnology Using Strand-Displacement Reactions. *Nat. Chem.* **2011**, *3*, 103−113.
(9) Seelig, G.; Soloveichik, D.; Zhang, D. Y.; Winfree, E. Enzyme-Free Nucleic Acid Logic Circuits. *Science* **2006**, *314*, 1585−1588.
(10) Han, D.; Wu, C.; You, M.; Zhang, T.; Wan, S.; Chen, T.; Qiu, L.; Zheng, Z.; Liang, H.; Tan, W. A cascade reaction network mimicking the basic functional steps of adaptive immune response. *Nat. Chem.* **2015**, *7*, 835−841.
(11) Hemphill, J.; Deiters, A. DNA computation in mammalian cells: microRNA logic operations. *J. Am. Chem. Soc.* **2013**, *135*, 10512−10518.
(12) Rinaudo, K.; Bleris, L.; Maddamsetti, R.; Subramanian, S.; Weiss, R.; Benenson, Y. A universal RNAi-based logic evaluator that operates in mammalian cells. *Nat. Biotechnol.* **2007**, *25*, 795−801.
(13) Montagne, K.; Gines, G.; Fujii, T.; Rondelez, Y. Boosting functionality of synthetic DNA circuits with tailored deactivation. *Nat. Commun.* **2016**, *7*, 13474.
(14) Johnson, D. S.; Mortazavi, A.; Myers, R. M.; Wold, B. Genome-Wide Mapping of in vivo Protein-DNA Interactions. *Science* **2007**, *316*, 1497−1502.
(15) Mcadams, H. H.; Shapiro, L. Circuit simulation of genetic networks. *Science* **1995**, *269*, 650−656.
(16) Stricker, J.; Cookson, S.; Bennett, M. R.; Mather, W. H.; Tsimring, L. S.; Hasty, J. A fast, robust and tunable synthetic gene oscillator. *Nature* **2008**, *456*, 516−519.
(17) Brown, C. W.; Lakin, M. R.; Horwitz, E. K.; Fanning, M. L.; West, H. E.; Stefanovic, D.; Graves, S. W. Signal Propagation in Multi-Layer DNAzyme Cascades Using Structured Chimeric Substrates. *Angew. Chem., Int. Ed.* **2014**, *53*, 7183−7187.
(18) Zhang, Z. X.; Balogh, D.; Wang, F. A.; Sung, S. Y.; Nechushtai, R.; Willner, I. Biocatalytic Release of an Anticancer Drug from Nucleic-Acids-Capped Mesoporous $SiO_2$ Using DNA or Molecular Biomarkers as Triggering Stimuli. *ACS Nano* **2013**, *7*, 8455−8468.
(19) Wang, F. A.; Freage, L.; Orbach, R.; Willner, I. Autonomous replication of nucleic acids by polymerization/nicking enzyme/DNAzyme cascades for the amplified detection of DNA and the aptamer-cocaine complex. *Anal. Chem.* **2013**, *85*, 8196−8203.
(20) Lu, C. H.; Wang, F. A.; Willner, I. $Zn^{2+}$-ligation DNAzyme-driven enzymatic and nonenzymatic cascades for the amplified detection of DNA. *J. Am. Chem. Soc.* **2012**, *134*, 10651−10658.
(21) Han, D.; Zhu, Z.; Wu, C.; Peng, L.; Zhou, L.; Gulbakan, B.; Zhu, G.; Williams, K. R.; Tan, W. A Logical molecular circuit for programmable and autonomous regulation of protein activity using DNA aptamer-protein interactions. *J. Am. Chem. Soc.* **2012**, *134*, 20797−20804.
(22) Ranallo, S.; Prévost-Tremblay, C. P.; Idili, A.; Vallée-Bélisle, A. V.; Ricci, F. Antibody-powered nucleic acid release using a DNA-based nanomachine. *Nat. Commun.* **2017**, *8*, 15150.
(23) Elbaz, J.; Lioubashevski, O.; Wang, F. A.; Remacle, F.; Levine, R. D.; Willner, I. DNA computing circuits using libraries of DNAzyme subunits. *Nat. Nanotechnol.* **2010**, *5*, 417−422.
(24) Li, J. M.; Johnson-Buck, A. J.; Yang, Y. R.; Shih, W. M.; Yan, H.; Walter, N. G. Exploring the speed limit of toehold exchange with a cartwheeling DNA acrobat. *Nat. Nanotechnol.* **2018**, *13*, 723−729.
(25) Meijer, L. H. H.; Joesaar, A.; Steur, E.; Engelen, W.; van Santen, R. A.; Merkx, M.; de Greef, T. F. A. Hierarchical control of enzymatic actuators using DNA-based switchable memories. *Nat. Commun.* **2017**, *8*, 1117.
(26) Chen, X.; Briggs, N.; McLain, J. R.; Ellington, A. D. Stacking nonenzymatic circuits for high signal gain. *Proc. Natl. Acad. Sci. U. S. A.* **2013**, *110*, 5386−5391.
(27) Chen, Y. J.; Dalchau, N.; Srinivas, N.; Phillips, A.; Cardelli, L.; Soloveichik, D. G.; Seelig, G. Seelig, Programmable chemical controllers made from DNA. *Nat. Nanotechnol.* **2013**, *8*, 755−762.
(28) Zhang, D. Y.; Winfree, E. Robustness and modularity properties of a non-covalent DNA catalytic reaction. *Nucleic Acids Res.* **2010**, *38*, 4182−4197.
(29) Srinivas, N.; Ouldridge, T. E.; Sulc, P.; Schaeffer, J. M.; Yurke, B.; Louis, A. A.; Doye, J. P. K.; Winfree, E. On the biophysics and kinetics of toehold-mediated DNA strand displacement. *Nucleic Acids Res.* **2013**, *41*, 10641−10658.
(30) Zhang, D. Y.; Turberfield, A. J.; Yurke, B.; Winfree, E. Engineering entropy-driven reactions and networks catalyzed by DNA. *Science* **2007**, *318*, 1121−1125.
(31) Qian, L.; Winfree, E.; Bruck, J. Neural network computation with DNA strand displacement cascades. *Nature* **2011**, *475*, 368−372.
(32) Zhang, D. Y.; Winfree, E. Control of DNA strand displacement kinetics using toehold exchange. *J. Am. Chem. Soc.* **2009**, *131*, 17303−17314.
(33) Collins, M. L.; Irvine, B.; Tyner, D.; Fine, E.; Zayati, C.; Chang, C. A.; Horn, T.; Ahle, D.; Detmer, J.; Shen, L. P.; Kolberg, J.; Bushnell, S.; Urdea, M. S.; Ho, D. D. A branched DNA signal amplification assay for quantification of nucleic acid targets below 100 molecules/ml. *Nucleic Acids Res.* **1997**, *25*, 2979−2984.
(34) Capaldi, S.; Getts, R. C.; Jayasena, S. D. Signal amplification through nucleotide extension and excision on a dendritic DNA platform. *Nucleic Acids Res.* **2000**, *28*, No. e21.
(35) Genot, A. J.; Bath, J.; Turberfield, A. J. Reversible Logic Circuits Made of DNA. *J. Am. Chem. Soc.* **2011**, *133*, 20080−20083.
(36) Qian, L.; Winfree, E. Scaling Up Digital Circuit Computation with DNA Strand Displacement Cascades. *Science* **2011**, *332*, 1196−1201.
(37) Srinivas, N.; Parkin, J.; Seelig, G.; Winfree, E.; Soloveichik, D. Enzyme-free nucleic acid dynamical systems. *Science* **2017**, *358*, No. eaal2052.
(38) Kishi, J. Y.; Schaus, T. E.; Gopalkrishnan, N.; Xuan, F.; Yin, P. Programmable autonomous synthesis of single-stranded DNA. *Nat. Chem.* **2018**, *10* (2), 155−164.
(39) Zhang, D. Y.; Hariadi, R. F.; Choi, H. M. T.; Winfree, E. Integrating DNA strand-displacement circuitry with DNA tile self-assembly. *Nat. Commun.* **2013**, *4*, 1965.
(40) Wickham, S. F. J.; Endo, M.; Katsuda, Y.; Hidaka, K.; Bath, J.; Sugiyama, H.; Turberfield, A. J. Direct observation of stepwise movement of a synthetic molecular transporter. *Nat. Nanotechnol.* **2011**, *6*, 166−169.
(41) DelRosso, N.; Hews, S.; Spector, L.; Derr, N. D. A Molecular circuit regenerator to implement iterative strand displacement operations. *Angew. Chem., Int. Ed.* **2017**, *56*, 4443−4446.
(42) Garg, S.; Shah, S.; Bui, H.; Song, T.; Mokhtar, R.; Reif, J. Renewable Time-Responsive DNA Circuits. *Small* **2018**, *14*, 1801470.
(43) Song, X.; Eshra, A.; Dwyer, C.; Reif, J. Renewable DNA seesaw logic circuits enabled by photoregulation of toehold-mediated strand displacement. *RSC Adv.* **2017**, *7*, 28130−28144.
(44) Weitz, M.; Kim, J.; Kapsner, K.; Winfree, E.; Franco, E.; Simmel, F. C. Diversity in the dynamical behaviour of a compartmentalized programmable biochemical oscillator. *Nat. Chem.* **2014**, *6*, 295−302.
(45) Fujii, T.; Rondelez, Y. Predator−prey molecular ecosystems. *ACS Nano* **2013**, *7*, 27−34.
(46) Genot, A. J.; Baccouche, A.; Sieskind, R.; Aubert-Kato, N.; Bredeche, N.; Bartolo, J. F.; Taly, V.; Fujii, T.; Rondelez, Y. High-resolution mapping of bifurcations in nonlinear biochemical circuits. *Nat. Chem.* **2016**, *8*, 760−767.
(47) Zou, B. J.; Ma, Y. J.; Wu, H. P.; Zhou, G. H. Ultrasensitive DNA Detection by Cascade Enzymatic Signal Amplifi- cation Based on Afu Flap Endonuclease Coupled with Nicking Endonuclease. *Angew. Chem., Int. Ed.* **2011**, *50*, 7395−7398.
(48) Song, T. Q.; Gopalkrishnan, N.; Eshra, A.; Garg, S.; Mokhtar, R.; Bui, H.; Chandran, H.; Reif, J. Improving the Performance of


DOI: 10.1021/jacs.9b07521
J. Am. Chem. Soc. 2019, 141, 17189−17197

DNA Strand Displacement Circuits by Shadow Cancellation. *ACS Nano* **2018**, *12*, 11689−11697.
(49) Bui, H.; Shah, S.; Mokhtar, R.; Song, T. Q.; Garg, S.; Reif, J. Localized DNA Hybridization Chain Reactions on DNA Origami. *ACS Nano* **2018**, *12*, 1146−1155.
(50) Wang, B.; Thachuk, C.; Ellington, A. D.; Winfree, E.; Soloveichik, D. Effective design principles for leakless strand displacement systems. *Proc. Natl. Acad. Sci. U. S. A.* **2018**, *115*, E12182−E12191.



DOI: 10.1021/jacs.9b07521
*J. Am. Chem. Soc.* 2019, 141, 17189−17197